Published in final edited form as:
Mol Cancer Res. 2015 January ; 13(1): 197–207. doi:10.1158/1541-7786.MCR-14-0118.

Annexin 2-CXCL12 Interactions Regulate Metastatic Cell Targeting and Growth in the Bone Marrow

Younghun Jung[1], **Jingcheng Wang**[1], **Eunsohl Lee**[1], **Samantha McGee**[1], **Janice E. Berry**[1], **Kenji Yumoto**[1], **Jinlu Dai**[2], **Evan T. Keller**[2], **Yusuke Shiozawa**[1], and **Russell S. Taichman**[1,*]

[1]Department of Periodontics and Oral Medicine, University of Michigan School of Dentistry, Ann Arbor, MI 48109, USA

[2]Department of Urology and Pathology, University of Michigan School of Medicine, Ann Arbor, MI, USA

Abstract

A nnexin 2 (ANXA2) plays a critical role in hematopoietic stem cell (HSC) localization to the marrow niche. In part, ANXA2 supports HSCs by serving as an anchor for stromal-derived factor-1 (CXCL12/SDF-1). Recently it was demonstrated that prostate cancer (PCa) cells, like HSCs, use ANXA2 to establish metastases in marrow. The present study determined the capacity of ANXA2 expression by bone marrow stromal cells (BMSC) to facilitate tumor recruitment and growth through ANXA2-CXCL12 interactions. Significantly more CXCL12 was expressed by BMSC$^{Anxa2+/+}$ compared to BMSC$^{Anxa2-/-}$ resulting in more PCa cells migrating and binding to BMSC$^{Anxa2+/+}$ than BMSC$^{Anxa2-/-}$, and these activities were reduced when CXCL12 interactions were blocked. To further confirm that BMSC signaling through ANXA2-CXCL12 plays a critical role in tumor growth, immunocompromised SCID mice were subcutaneously implanted with human PCa cells mixed with BMSC$^{Anxa2+/+}$ or BMSC$^{Anxa2-/-}$. Significantly larger tumors grew in the mice when the tumors were established with BMSC$^{Anxa2+/+}$ compared to the tumors established with BMSC$^{Anxa2-/-}$. In addition, fewer PCa cells underwent apoptosis when co-cultured with BMSC$^{Anxa2+/+}$ compared to BMSC$^{Anxa2-/-}$, and similar results were obtained in tumors grown *in vivo*. Finally, significantly more vascular structures were observed in the tumors established with the BMSC$^{Anxa2+/+}$ compared to the tumors established with BMSC$^{Anxa2-/-}$. Thus, ANXA2-CXCL12 interactions play a crucial role in the recruitment, growth, and survival of PCa cells in the marrow.

Implications—The tumor microenvironment interaction between ANXA2-CXCL12 is critical for metastatic phenotypes and may impact chemotherapeutic potential.

Keywords

Prostate cancer; BMSC; ANXA2; CXCL12; Tumor growth

[*]Corresponding Author: Russell S. Taichman, D.M.D., D.M.Sc., Department of Periodontics and Oral Medicine, University of Michigan School of Dentistry, 1011 North University Avenue, Ann Arbor, MI 48109, USA, Phone: 1-734-764-9952, Fax: 1-734-763-5503, rtaich@umich.edu.

Introduction

Prostate cancer (**PCa**) is the second leading cause of cancer deaths in American males (1, 2). The high mortality rate is due mainly to the spread of malignant cells to many tissues including bone (3, 4). At the single cell level, the multistep process of metastasis is very inefficient, where less than ~2% of disseminated tumor cells (**DTCs**) as estimated to form micrometastasis and fewer still (~0.02%) develop into macrometastasis (5). In part, a barrier for DTCs to form clinically relevant metastases is not only the ability to survive in the circulation during dissemination, but also the ability to home and to engage in a safe environment, which can immediately support their survival. We recently reported that DTCs target and engage the hematopoietic stem cell (**HSC**) niche to establish metastases in marrow (6). While the nature and the components of the HSC niche remain controversial, significant evidence suggests that cells of the osteoblastic lineage, adipocytes, osteoclasts, osteomacs and endothelial cells aid in the development and organization of the HSC niche (7–9).

Bone marrow stromal cells (**BMSC**) are a heterogeneous population of cells, which also are known to contribute to the generation of the HSC niche. There is growing evidence that a subpopulation of BMSCs has progenitor and/or stem like activities which are capable of locally generating multiple connective tissue lineages under conditions of stress or wound repair (e.g. endothelial, adipocytic, osteoblastic, cartilage, and muscle cells) (7–9). Although still controversial, if BMSCs are mobilized or injected into the circulation, BMSCs may participate in tissue repair at distant organs (9). In the context of tumors, when BMSCs are localized in tumor beds, cytokine cross-talk leads to the emergence of an increasingly aggressive tumor phenotype (10–17).

Two important signal transducers in the bone marrow niche are stromal derived factor-1 (**SDF-1** or **CXCL12**) and annexin 2 (**ANXA2**) (18–30). CXCL12 is a central regulator of HSC homing and recruitment into marrow and HSC mobilization into the circulation. Indeed, blockage of CXCL12 or its receptor prevents HSC homing, or mobilizes niche-bound HSC into the circulation (18–24). ANXA2, on the other hand, likely serves as an adhesion molecule, facilitating HSC binding to the osteoblastic niche (25). Critically, it has been shown that CXCL12 and ANXA2 directly bind to one another, and this interaction facilitates hematopoietic progenitor cell migration in response to CXCL12 (26). In fact, loss of ANXA2 is associated with decreased levels of CXCL12 in marrow. Likewise, CXCL12 and ANXA2 play similar roles in recruiting and localizing tumor cells into the HSC niche (27–30).

In the present study, we explored whether ANXA2 facilitates metastasis and growth of PCa through its interactions with CXCL12. We demonstrate that ANXA2-expressing BMSCs express more CXCL12 than do BMSCs that do not express ANXA2, and the production of these two proteins increases the recruitment of PCa cells into the marrow niche. In addition, CXCL12 produced by ANXA2-expressing BMSCs promotes PCa proliferation, protects PCa from chemotherapy-induced apoptosis, and increases the development of vascular structures. Our results suggest that ANXA2 and CXCL12 interactions facilitate the recruitment, growth, and survival of PCa cells in marrow.

Materials and Methods

Cell cultures

The human PCa cell line PC3 was obtained from the American Type Culture Collection (Rockville, MD). C4-2B, the metastatic subline of the prostate cancer cell line LNCap, were originally isolated from a lymph node of a patient with disseminated bony and lymph node involvement. Luciferase expressing PCa cell lines ($PC3^{Luc}$ and $C4\text{-}2B^{Luc}$ cells) and GFP expressing PCa cell lines ($PC3^{GFP}$ and $C4\text{-}2B^{GFP}$ cells) were established by lentiviral transduction. Human bone marrow endothelial cells (**HBMEC**) were isolated from a normal Caucasian male, and immortalized with SV40 large T-antigen (31). PCa cells and HBMEC were grown in RPMI 1640 (Invitrogen, Carsbad, CA) supplemented with 10% fetal bovine serum (**FBS**) and 1% penicillin/streptomycin (**P/S**).

Bone marrow stromal cells (**BMSCs**) from $Anxa2^{+/+}$ or $Anxa2^{-/-}$ mice (five to seven-week old) were used for this study. Dr. K. A. Hajjar (Weill Medical College of Cornell University, New York, NY) graciously provided our laboratory with a pair of the homozygous $Anxa2^{-/-}$ mice for breeding (32). After sacrifice, marrow was flushed from femurs and tibias of both $Anxa2^{+/+}$ and $Anxa2^{-/-}$ mice with α-MEM (Invitrogen) containing 2% FBS, and cultured in α-MEM containing 15% heat-inactivated FBS and 1% P/S to generate primary BMSCs. Once confluent, the cells were passaged 2–3 times with trypsin to minimize macrophage contamination. Subsequently, repopulated BMSCs was obtained, and the cells were cultured in α-MEM containing 10% heat-inactivated FBS and 1% P/S. These isolated cells were termed as $BMSC^{Anxa2+/+}$ and $BMSC^{Anxa2-/-}$. For differentiation assays, mouse primary BMSCs were cultured in adipogenic, osteogenic, or chondrogenic conditions for 2 weeks, fixed and stained for identification with Alizarin Red S, Oil Red O, and Alcian Blue, respectively.

Proliferation assays

$BMSC^{Anxa2+/+}$ or $BMSC^{Anxa2-/-}$ (1×10^5 cells/well) was seeded onto 12-well culture plates for 24 hours and $PC3^{Luc}$ cells (1×10^5 cells/well) were directly co-cultured with $BMSC^{Anxa2+/+}$ or $BMSC^{Anxa2-/-}$ for 48 hours. The amount of luciferase in these cultures was measured by Dual-Luciferase Reportor Assay kit (cat. E1910, Promega, Madison, WI) and detected using a luminometer (BD Monolight™ 2010, BD Biosciences, San Jose, CA).

Adhesion assays

$BMSC^{Anxa2+/+}$ or $BMSC^{Anxa2-/-}$ were plated onto 96-well plates at a concentration of 1×10^4 cells/100μl/well in growth medium, and the cultures were incubated for 2 days. PCa cells were labeled with 2.5 mg/ml of the lipophilic dye carboxyfluorescein diacetate (CFDA, cat. V12883, Molecular Probes, Eugene, OR) in RPMI for 30 min at 37°C, and washed in PBS. Thereafter, PCa cells (1×10^4 cells/well) were added to each well, and were left for 30 min at room temperature to allow binding to BMSCs. In some cases, adhesion assays of PCa cells to BMSCs were done in the presence or absence of function blocking antibody to ANXA2 (cat. 610069, BD Pharmingen, San Diego, CA), with matched IgG as an antibody control. Total fluorescence per well was determined initially, followed by washing wells with PBS to quantify fluorescence for PCa cells adherent to BMSCs.

Transwell chemotaxis assays

BMSC$^{Anxa2+/+}$ or BMSC$^{Anxa2-/-}$ (1×10^5 cells/well) were seeded onto 24-well culture plates. PCa cells or HBMECs were labeled with 2.5μg/ml of CFDA as described above. PCa cells or HBMECs were resuspended in serum-free RPMI 1640 and equilibrated for 10 min at 37°C. CFDA-labelled PCa cells or HBMECs were loaded into the top chambers of 8μm Transwell® microporous membrane 24-well plates (cat. 3422, Costar Corp, Cambridge, MA). 650μl of conditioned medium (**CM**) from 3 day cultures of BMSC$^{Anxa2+/+}$ or BMSC$^{Anxa2-/-}$ (1×10^5 cells/well) was added into the bottom well. The plates were incubated at 37°C for 3 hours. At the termination of the experiments, the intensity of fluorescence in the lower chamber, indicating the number of cells which had migrated cells, was determined by plate reader (Molecular Probes, Eugene, OR). In some cases, migration of PCa cells to CM isolated from BMSCs was analyzed in the presence of neutralizing anti-CXCL12 monoclonal antibodies (120μg/ml, cat. MAB310, R&D Systems, Minneapolis, MN) or AMD3100, a selective CXCR4 antagonist (4ng/ml, cat. A5602, Sigma, St. Louis, MO).

Cell death assays

BMSC$^{Anxa2+/+}$ or BMSC$^{Anxa2-/-}$ (1×10^5 cells/well) were seeded onto 12-well culture plates for 24 hours. GFP expressing PCa cells (1×10^5 cells/well) were added to the wells and cultured together with the BMSCs for 48 hours prior to the addition of the anticancer drug, taxotere (1μg/ml, cat. NDC0409-0201-10, Hospira, Lake Forest, IL) for an additional 48 hours. Additionally, HBMECs (1×10^5 cells/well) were seeded onto 12-well culture plates for 24 hours and the cells were treated with ANXA2 (1μg/ml, cat. 11-511-248-344, Genway Biotech, San Diego, CA) or CXCL12 (200ng/ml, cat. 350-NS, R&D System) for 48 hours. Apoptosis in these cultures was measured by flow cytometry (FACSAria dual laser flow-cytometer, Becton Dickinson, Mountainview, CA) using PE Annexin V Apoptosis Detection Kit I (cat. 559763, BD Biosciences, San Jose, CA). Assays were performed in triplicate and the results are representative of three independent experiments. In tissue sections from mice inoculated with human PCa, apoptosis of PCa cells and endothelial cells in the tumors was measured by TUNEL staining (cat. 11684817910, Roche, Branford, CT).

Quantitative RT-PCR

Total RNA was extracted using the RNeasy mini or micro kit (Qiagen, Valencia, CA). cDNA was established using a First-Strand Synthesis Kit (Invitrogen). Quantitative PCR was performed on an ABI 7700 sequence detector (Applied Biosystems) using TaqMan Universal PCR Master Mix Kit (Applied Biosystems) according to the directions of manufacturer. TaqMan MGB probes (Applied Biosystems) were as follows: human *Anxa2r* (Hs01588662_s1) and human *Cxcr4* (Hs00237052_m1). *β-actin* (Hs99999903_m1) was used as an internal control for the normalization of target gene expression.

ELISAs

BMSC$^{Anxa2+/+}$or BMSC$^{Anxa2-/-}$ (1×10^5 cells/well) were cultured in 12-well culture plates for 48 hours. An antibody sandwich ELISA was used to evaluate CXCL12 levels in the CM

by the modification of directions of manufacturer (R&D Systems). CXCL12 secretion levels were normalized to total cell numbers.

Immunostaining

Cells and tumor sections were used for immunostaining. Cells were fixed with 10% neutral buffered formalin (cat. HT501320, Sigma) and permeabilized with PBT (1:500 dilution of Triton-X100 in PBS). Tumor sections were deparaffinized, hydrated, and then blocked with Image-iT FX signal enhancer (cat. I36933, Life Technology, Madison, WI) for 30 min and incubated for 2 hours at room temperature with primary antibodies combined with reagents of Zenon Alexa Fluor 488 (green) or 555 (red) labeling kit (Life Technology). Polyclonal anti-ANXA2 (cat. 610069, 1:25 dilution, BD Pharmingen), polyclonal anti-CXCL12 (cat. ab25117, 1:100 dilution, Abcam, Cambridge, MA), monoclonal anti-HLA (cat. 311402, 1:50 dilution, BioLegend, San Diego, CA), CD31 (cat. ab32457, 1:100 dilution, Abcam), monoclonal p-AKT (cat. ab81283, 1:100 dilution, Abcam), and monoclonal anti-AKT (cat. ab32505, 1:100 dilution, Abcam) were used as primary antibody. After washing with PBS, tumor sections were mounted with ProLong Gold antifade reagent with DAPI (cat. P36931, Invitrogen). Images were taken with Olympus FV-500 confocal microscope. In some cases, the tumor sections were stained by TUNEL staining (cat. 11684817910, Roche).

Western blots

PC3 cells (89–90% confluent) were cultured in 6 well plates in RPMI (1ml) without FBS for 18 hours. After serum starvation, the cells were treated with ANXA2 (1μg/ml), CXCL12 (200ng/ml), or combination of ANXA2 (1μg/ml) and CXCL12 (200ng/ml) for 30 min at 37°C. Whole cell lysates were prepared from cells, separated on 10% SDS-polyacrylamide gel and transferred to PVDF membrane. The membranes were first incubated with 5% milk for 1 hour prior to the addition of antibodies to p-AKT (cat. 9271, 1:1,000 dilution, Cell Signaling, Danvers, MA), and AKT (cat. 9272, 1:1,000 dilution, Cell Signaling) followed by overnight at 4°C. Subsequently the blots were incubated with peroxidase-coupled anti-rabbit IgG secondary antibody (cat. 7074, 1:2,000 dilution, Cell Signaling) for 1 hour, and protein expression was detected with SuperSignal West Dura Chemiluminescent Substrate (cat. Prod 34075, Thermo Scientific, Rockford, IL).

Subcutaneous tumor growth

To evaluate tumor growth, subcutaneous (*s.c.*) tumors were established. The $PC3^{luc}$ cells (2×10^5 cells) mixed with $BMSC^{Anxa2+/+}$ or $BMSC^{Anxa2-/-}$ (2×10^5 cells) in Collagen I (cat. 354236, BD Bioscience, Bedford, MA) were injected *s.c.* into 5–7 week-old male SCID mice. Mice were imaged weekly by bioluminescence imaging (BLI). After 5 weeks the animals were sacrificed and tumors were prepared for histology.

Intratibial tumor growth

To evaluate tumor growth in bone marrow, $PC3^{luc}$ (1×10^5 cells) or $C4\text{-}2B^{luc}$ (3×10^5 cells) were inoculated intratibially (*i.t.*) into 5–7 week-old male SCID mice. For intratibial injection, mice were anesthetized with 2.5% isofluorane/air, and both legs were cleaned with betadine and 70% ethanol. The knee was flexed and a 27-G3/8-inch needle was inserted into

the proximal end of right tibia followed by injection of 20 μl single-cell suspensions of PCa cells. Tumors were allowed to become established for 5 weeks. All animals were sacrificed at week 5 and tibiae with tumors were collected for histology.

Statistical analyses

Results are presented as mean ± standard deviation (s.d.). Significance of the difference between two measurements was determined by unpaired Student's *t*-test, and multiple comparisons were evaluated by the Newman-Keuls multiple comparison test. Values of $p < 0.05$ were considered significant.

Results

ANXA2 and CXCL12 expression are correlated in the bone marrow environment

We examined the extent to which ANXA2 expression is correlated with CXCL12 expression in the long bones of wild-type and *Anxa2* knocked-out mice. CXCL12 expression was robustly expressed in marrow of wild-type mice compared to ANXA2 deficient mice (Fig. 1A). *In vitro*, more CXCL12 expressing cells were identified in BMSCs derived from wild-type mice ($BMSC^{Anxa2+/+}$) compared to BMSCs derived from *Anxa2* knocked-out mice ($BMSC^{Anxa2-/-}$) (Fig. 1B). CXCL12 protein levels in the conditioned medium (CM) of the $BMSC^{Anxa2+/+}$ were significantly greater than those generated by $BMSC^{Anxa2-/-}$ cultures (Fig. 1C). The findings suggest that ANXA2 expression by BMSCs is correlated with CXCL12 expression in bone marrow microenvironment.

Interactions between ANXA2 and CXCL12 by BMSCs contribute to PCa cell adhesion and migration

To test whether expression of the ANXA2 receptor (*Anxa2r*) and the receptor for CXCL12, *Cxcr4*, are correlated mRNA levels were quantified using qRT-PCR. Significantly higher levels of *Anxa2r* or *Cxcr4* expression were observed in the bone homing PCa cell lines PC3 and C4-2B, compared with human BMSCs (Fig. 2A and B). Studies were next performed to determine if ANXA2 serves as an adhesion molecule for PCa cell binding to BMSCs. As shown in Fig. 2C, the binding of PCa cells to $BMSC^{Anxa2+/+}$ was significantly greater than the binding of PCa cells to $BMSC^{Anxa2-/-}$. When the experiments were repeated in the presence of a function of blocking antibody targeting ANXA2, significant reductions of PCa binding to $BMSC^{Anxa2+/+}$ was observed (Fig. 2D).

CXCL12 is a key regulator of hematopoietic stem cell migration and tumor metastasis into the marrow. As ANXA2 expression is linked to expression of CXCL12, we next performed migration assays of PCa cells in response to $BMSC^{Anxa2+/+}$ or $BMSC^{Anxa2-/-}$. For these studies PCa cells were added to the upper chamber of a migration assay dish with CM derived from $BMSC^{Anxa2+/+}$ or $BMSC^{Anxa2-/-}$ were added to the bottom chambers. More PCa cells migrated towards the CM derived from $BMSC^{Anxa2+/+}$ than they did towards $BMSC^{Anxa2-/-}$ CM (Fig. 2E). When the experiments were performed in the presence of neutralizing anti-CXCL12 antibody or AMD3100, a selective CXCR4 antagonist, significant reductions of PCa migrating to $BMSC^{Anxa2+/+}$ CM were observed (Fig. 2F). These data

suggest that PCa move towards CXCL12 secreted by BMSCs. These observations suggest that ANXA2 and CXCL12 participate in tissue localization of PCa.

Expression of ANXA2 and CXCL12 by BMSCs contributes to PCa cell growth

Next, we evaluated whether or not the interaction of ANXA2 and CXCL12 plays a role in PCa tumor growth *in vitro*. Here, PCa cells ($PC3^{Luc}$; 1×10^5) were co-cultured with $BMSC^{Anxa2+/+}$ or $BMSC^{Anxa2-/-}$ (1×10^5) for 48 hours in 12-well culture plates. Thereafter, luciferase activity was measured by Dual-Luciferase Reporter Assay kit to monitor PCa growth. More luciferase activity was observed when the tumor cells were cocultured with $BMSC^{Anxa2+/+}$ than with $BMSC^{Anxa2-/-}$ (Fig. 3A).

Based on the *in vitro* studies, we examined whether there are differences in the ability of BMSCs to support PCa growth *in vivo* linked to expression of ANXA2 and CXCL12. For these studies, tumors were established by *s.c.* injecting $PC3^{Luc}$ cells (2×10^5) mixed with $BMSC^{Anxa2+/+}$ or $BMSC^{Anxa2-/-}$ (2×10^5) in type I collagen into 5–7 week-old male SCID mice. Bioluminescent imaging at 5 week was used to monitor tumor growth. Significantly larger tumor growth occurred when the tumor cells were mixed with $BMSC^{Anxa2+/+}$ compared with tumors established with $BMSC^{Anxa2-/-}$ (Fig. 3B and C). To further test the growth of PCa cells in the bone marrow, tumors were established by injecting $PC3^{luc}$ (1×10^5 cells) or $C4\text{-}2B^{luc}$ (3×10^5 cells) intratibially into 5–7 week-old male SCID mice. We found that PCa cells are able to grow in bone marrow, and these tumor cells interact to ANXA2 or CXCL12-expressing osteoblast cells on the bone surface in marrow (Fig. 3D). To explore the molecular mechanisms whereby ANXA2 and CXCL12 regulate tumor growth, we examined whether ANXA2 alone, CXCL12 alone or in combination of ANXA2 and CXCL12 activates AKT in PCa cells. For these investigations, PCa cells were treated with ANXA2 and/or CXCL12 and phosphorylation of AKT was evaluated by western blot. The data demonstrate that ANXA2 or CXCL12 alone highly induces AKT phosphorylation in PC3 cells, and the combination of ANXA2 and CXCL12 significantly enhances activation of AKT phosphorylation (Fig. 3E). To validate the *in vitro* results, we examined induction of AKT phosphorylation on the tumors generated in Fig. 3B. The immunofluorescence data demonstrate that the expression levels of p-AKT was significantly enhanced in the tumor cells were mixed with $BMSC^{Anxa2+/+}$ compared with tumors established with $BMSC^{Anxa2-/-}$ or tumors alone (Fig. 3F). These data suggested that ANXA2 and CXCL12 facilitate the PCa growth via the AKT pathway.

Expression of ANXA2 and CXCL12 by BMSCs contributes to protection from chemotherapy-induced apoptosis

PCa cells are known to develop resistance to chemotherapies, particularly in marrow. To explore the role that ANXA2 and CXCL12 play in this process, co-cultures of BMSCs and PCa cells were evaluated by FACS for Annexin V staining (Fig. 4). Apoptosis levels for PCa cells cocultured with $BMSC^{Anxa2+/+}$ were lower than when PCa cells were cultured alone or with $BMSC^{Anxa2-/-}$. Further protection from apoptosis was noted when the microtubule inhibiting drug taxotere was included in the cultures (Fig. 4A and B). To evaluate if these *in vitro* studies are also relevant to our *in vivo* studies, TUNEL staining was next performed on the tumors generated in Fig. 3B. Fewer apoptotic tumor cells were found

in the tumors established with PC3^{Luc} and BMSC$^{Anxa2+/+}$ compared with tumors generated from PC3^{Luc} mixed with BMSCs$^{Anxa2-/-}$ (Fig. 4C and D). Together the data suggest that ANXA2 and CXCL12 expression by BMSCs are likely to play a role in the resistance of PCa cells to chemotherapy.

Expression of ANXA2 and CXCL12 by BMSCs contributes to the generation of vascular structures in tumors

To determine if ANXA2 and CXCL12 contribute to endothelial cell recruitment into tumor beds, migration by endothelial cells in response to CM isolated from BMSCs was evaluated. When human bone marrow endothelial cells (HBMEC) were added to the upper chamber of the culture dish with BMSCs cell CM present in the bottom, fewer HBMEC migrated towards BMSC$^{Anxa2-/-}$ CM compared with BMSC$^{Anxa2+/+}$ CM. When the experiments were performed in the presence of AMD3100, significant reduction of HBMECs migrating to BMSC$^{Anxa2+/+}$ or BMSC$^{Anxa2-/-}$ CM was observed (Fig. 5A). These data suggest that endothelial cells move towards CXCL12 secreted by ANXA2 expressing BMSCs and further suggest that ANXA2 and CXCL12 participate in tissue localization of endothelial cells. Next, immunostaining for CD31, a marker of endothelial cells, was performed on tumors generated by PC3 cells in combination with BMSC$^{Anxa2+/+}$ or BMSC$^{Anxa2-/-}$. Tumors established with PC3^{Luc} and BMSC$^{Anxa2+/+}$ demonstrated significantly larger and more abundant CD31-expressing blood vessels compare the tumors established with PC3 and BMSC$^{Anxa2-/-}$ (Fig. 5B and C).

One possible mechanism which may account for the observation that more CD31 endothelial cells were present in tumors generated with BMSC$^{Anxa2+/+}$, is that BMSCs enhances endothelial cell survival. To test this possibility, endothelial cells were treated with ANXA2 and CXCL12 alone or in combination, and survival was determined by FACS for Annexin V staining as a measurement of apoptosis. We found that fewer HBMECs underwent apoptosis in the presence of ANXA2 and/or CXCL12 (Fig. 5D). TUNEL staining was next used to examine endothelial cell survival in tumors. Tumors established with PC3^{Luc} and BMSC$^{Anxa2+/+}$ had fewer apoptotic endothelial cells compared with tumors established with PC3^{Luc} mixed with BMSC$^{Anxa2-/-}$ (Fig. 5E and F). Together the data suggest that ANXA2-mediated CXCL12 in BMSCS plays an important role in sustaining vascular structures.

Discussion

Recent studies suggest that niche cells in the bone marrow participate in the cellular and molecular events for the tumor progression and metastasis (5–9). In this study, we show ANXA2 and CXCL12 interactions produced by BMSCs facilitate PCa recruitment and proliferation, aid in protection of PCa cells from chemotherapy-induced apoptosis, and facilitate the generation of vascular structures in tumors. Together these data suggest that ANXA2 and CXCL12 interactions may be integral to tumor development in the marrow microenvironment.

The engagement of disseminated tumor cells (DTCs) to the bone marrow niche and the maintenance of these cells in the niche are essential steps to establish metastases. In this

context, ANXA2, an osteoblast-expressed adhesion molecule, may be a crucial docking signal (30). CXCL12 is a chemokine, which in addition to functioning as a secreted molecule is known to bind to extracellular matrix proteins (27–29). Previously, we and other groups have identified several factors that may be involved in establishing a tumor niche. We have shown that CXCL12 produced by the niche participates in the regulation of PCa metastasis (27–29), and we have also demonstrated that ANXA2 and its receptor ANXA2R regulate the localization and maintenance of PCa cells in the niche (30). More importantly, tumor cell metastases share molecular mechanisms which regulate HSC homing and localization to the bone marrow (27–30). Subsequently, we reported that ANXA2 and CXCL12 binds directly to each other, and these interactions facilitate hematopoietic progenitor cell migration in response to CXCL12 (26). We therefore hypothesized that ANXA2-expressing bone marrow stromal cells facilitate PCa metastasis and growth by inducing CXCL12. We found that ANXA2-expressing BMSCs express elevated levels of CXCL12, which increase the binding and recruitment of PCa cells into the marrow niche and promote PCa proliferation. Thus, a model can be envisioned in which CXCL12 facilitates the recruitment of DTCs to the niche, ANXA2 facilitates PCa engagement into the niche, where upon CXCL12 produced by the niche cells stimulates PCa growth. CXCL12 is known to play a central role in promoting the growth of tumor cells including ovarian carcinoma (33), small cell lung cancer (34), head and neck squamous cell carcinoma (35), pancreatic cancer (36), and prostate cancer (37). It has also been demonstrated that secreted CXCL12 induces PCa proliferation in *in vitro* (37–39), following activation of ERK1/2 and AKT pathways (34, 36, 37). We also found that ANXA2 and CXCL12 interactions effectively activate through AKT signaling pathways which, in many respects, have been linked to tumor growth.

In marrow, osteoblasts play important roles in the production of a mineralized matrix that serves as the basis of bone remodeling. Osteoblasts are also known to express many cell adhesion molecules, including ANXA2, which may facilitate bone activities. Recently it was demonstrated that ANXA2 regulates osteogenic differentiation, yet the molecular mechanisms remain unclear (40–42). Hypoxia and VEGF both induce ANXA2 expression by osteoblasts and endothelial cells through SRC and MEK kinase-dependent pathway (40). ANXA2 increases the mineralization of osteoblastic cells and alkaline phosphatase activity (41). ANXA2 also supports osteogenic differentiation of mesenchymal stem cells (MSCs), and further regulates both intramembrane and endochondral ossification in adolescent idiopathic scoliosis (AIS) (42). We have also reported that fewer osteoblasts are found in the long bone of *Anxa2* knocked-out (*Anxa2*$^{-/-}$) mice compared to wild-type (*Anxa2*$^{+/+}$) mice and, likewise, a decrease of bone phenotype markers (*Runx2*, osteocalcin, Collagen 1a) is seen in bones from these knock-out mice (data not shown). Critical to this report, lower CXCL12 expressing cells in BMSCs derived from *Anxa2* knocked-out mice (BMSC$^{Anxa2-/-}$) were identified compared to cells isolated from wild-type mice (BMSC$^{Anxa2+/+}$). As ANXA2 mediates osteogenic activities in marrow, the release of tumor-supporting activities from either osteoblasts or bone matrix may provide some clues to how ANXA2 regulates metastasis and CXCL12 signaling simply by providing lower levels of substrates or adhesive surfaces for DTCs to lodge. Alternatively, while the molecular mechanisms need to be further investigated, our data also suggest that an

ANXA2-deficient environment may lead to less osteoblastic regulation of bone remodeling, which ultimately results in a decrease of PCa tumor growth and survival in bone marrow. Both of these two possibilities are worthy of further study.

CXCL12 is known to regulate tumor cell apoptosis. CXCL12 may protect tumor cells from drug-induced apoptosis directly through the activation of antiapoptotic pathways, but also indirectly by modulating the adherence of cancer cells. CXCL12 mediates adhesion of small-cell lung cancer cells (SCLC) to marrow stromal cells and protects SCLC against drug-induced apoptosis (34). CXCL12 activates NF-kB, which inhibits radiation-induced tumor necrosis factor-α (TNF-α) production and tumor apoptosis (43, 44). Moreover, NF-kB signaling is involved in the expression of CXCR4, thus promoting tumor cell migration and metastasis (43–45). In this study, we found that more PCa cells survived when co-cultured with BMSC$^{Anxa2+/+}$ vs. co-culture with BMSC$^{Anxa2-/-}$ in *in vitro.* Similar results were obtained in *in vivo* studies, as fewer apoptotic cells were found in tumors established with BMSC$^{Anxa2+/+}$ vs. those with BMSC$^{Anxa2-/-}$ cells. In part, these results may be due to regulation of CXCL12 expression by ANXA2 or enhanced ability to localize CXCL12 to cell surfaces, which may be more efficient in activating cell functions than in a soluble form. Whether either of these two possibilities is responsible for how ANXA2 interacts with CXCL12 remains unclear and will require additional investigation.

Finally, migration, expansion and survival of vascular endothelial cells are essential for establishment of a functional network of angiogenesis. Ling *et al.* demonstrated that *Anxa2*-deficient mice have markedly impaired neoangiogenesis. This contributes to a failure to localize plasmin activity to the endothelial cell surface and a failure to activate selected matrix metalloproteinase (32). It has also been demonstrated that ANXA2-dependent plasmin generation in breast tumor is necessary to trigger the switch to neoangiogenesis, thereby stimulating tumor growth (46, 47). We found that PC3^{Luc} cells implanted with BMSC$^{Anxa2+/+}$ showed significantly more and larger CD31-expressing blood vessels compared to PC3^{Luc} mixed BMSC$^{Anxa2-/-}$ cells. It has also been demonstrated that CXCL12 stimulates the formation of capillary-like structures with human vascular endothelial cells (48–51). Recently, we demonstrated that PCa cells use CXCL12 and its receptors (CXCR4 and CXCR7) as key elements in metastasis and growth in bone, where CXCR4 signaling leads to an angiogenic switch (48–50). We have further demonstrated that CXCR4 signaling results in the activation of MAP and AKT pathways, which ultimately increases the secretion of VEGF and IL8 (48–50). More importantly, CXCR4 directly regulates blood vessel formation (48), due to inhibiting the secretion of the vascular inhibitor phophoglycerate kinase 1 (PGK1) (50). Thus, there are both direct and indirect mechanisms whereby ANXA2 and CXCL12 interactions may regulate tumor growth. Clearly, more studies are warranted.

In summary, this work provides further evidence for the role that ANXA2 and CXCL12 play in the tumor microenvironment, and specifically in PCa migration, growth, and survival in bone marrow. Our data also provide evidence that ANXA2 and CXCL12 regulate vascular formation in tumors. Together these studies suggest that ANXA2 and CXCL12 interactions facilitate a number of activities critical for tumor growth.

Supplementary Material

Refer to Web version on PubMed Central for supplementary material.

Acknowledgments

This work is directly supported by the National Institutes of Health (CA163124, CA093900, CA166307, CA069568, DK082481, MH095589 (Y.S. and R.S.T.), the Department of Defense (W81XWH-11-1-0636, PC130359, Y.S. and R.S.T.), the Prostate Cancer Foundation (Y.S and R.S.T). This research was supported in part by the National Institutes of Health through the University of Michigan's Cancer Center Support Grant (P30 CA046592) by the use of the following Cancer Center Core(s): Flow Cytometry, Microscopy and Imaging, Tissue & Molecular Pathology Cores. Logistical support was also received from the Dental School's Molecular Biology Core.

References

1. Pienta KJ, Esper PS. Risk factors for prostate cancer. [Review] [178 refs]. Annals of Internal Medicine. 1993; 118(10):793–803. [PubMed: 8470854]
2. Siegel R, Naishadham D, Jemal A. Cancer statistics. CA Cancer J Clin. 2012; 62:10–29. [PubMed: 22237781]
3. Koutsilieris M. Osteoblastic metastasis in advanced prostate cancer. Anticancer Research. 1993; 13(2):443–449. [PubMed: 8517661]
4. Jacobs SC. Spread of prostatic cancer to bone. Urology. 1983; 21(4):337–344. [PubMed: 6340324]
5. Honoki, K.; Fujii, H.; Tsujiuchi, T. Cancer Stem Cell Niche: The role of mesenchymal stem cells in tumor microenvironment. In: Shostak, Stanley, Prof, editor. Cancer Stem Cells-The Cutting Edge. Vol. 189. 2011.
6. Shiozawa Y, Pedersen EA, Havens AM, Jung Y, Mishra A, Joseph J, Kim JK, Patel LR, Ying C, Ziegler AM, Pienta MJ, Song J, Wang J, Loberg RD, Krebsbach PH, Pienta KJ, Taichman RS. Human prostate cancer metastases target the hematopoietic stem cell niche to establish footholds in mouse bone marrow. J Clin Invest. 2011; 121(4):1298–1312. [PubMed: 21436587]
7. Wels J, Kaplan RN, Rafii S, Lyden D. Migratory neighbors and distant invaders: tumor-associated niche cells. Genes Dev. 2008; 22:559–574. [PubMed: 18316475]
8. Taichman RS, Wang Z, Shiozawa Y, Jung Y, Song J, Balduino A, Wang J, Patel LR, Havens AM, Kucia M, Ratajczak MZ, Krebsbach PH. Prospective identification and skeletal localization of cells capable of multilineage differentiation in vivo. Stem Cells Dev. 2010; 19:1557–1570. [PubMed: 20446812]
9. Ziadloo A, Burks SR, Gold EM, Lewis BK, Chaudhry A, Merino MJ, Frenkel V, Frank JA. Enhanced homing permeability and retention of bone marrow stromal cells by noninvasive pulsed focused ultrasound. Stem Cells. 2012; 30(6):1216–1227. [PubMed: 22593018]
10. Studeny M, Marini FC, Champlin RE, Zompetta C, Fidler IJ, Andreeff M. Bone marrow-derived mesenchymal stem cells as vehicles for interferon-beta derivery into tumors. Cancer Res. 2002; 62:3603–3608. [PubMed: 12097260]
11. Dwyer RM, Potter-Beirne SM, Harrington KA, Lowery AJ, Hennessy E, Murphy JM, Barry FP, O'Brien T, Kerin MJ. Monocyte chemotactic protein-1 secreted by primary breast tumors stimulates migration of mesenchymal stem cells. Clin Cancer Res. 2007; 13:5020–5027. [PubMed: 17785552]
12. Hall B, Andreeff M, Marini F. The participation of mesenchymal stem cells in tumor stroma formation and their application as targeted-gene delivery vehicles. Handb Exp Pharmacol. 2007; 180:263–283. [PubMed: 17554513]
13. Mishra PJ, Mishra PJ, Glod JW, Banerjee D. Mesenchymal stem cells: flip side of the coin. Cancer Res. 2009; 69:1255–1258. [PubMed: 19208837]
14. Roorda BD, Elst At, Boer TG, Kamps WA, de Bont ES. Mesenchymal stem cells contribute to tumor cell proliferation by direct cell-cell contact interactions. Cancer Invest. 2010; 28(5):526–531. [PubMed: 20210526]

15. Abarrategi A, Marinas-Pardo L, Mirones I, Rincon E, Garcia-Castro J. Mesenchymal niches of bone marrow in cancer. Clin Transl Oncol. 2011; 13:611–616. [PubMed: 21865132]
16. Mi Z, Bhattacharya SD, Kim VM, Guo H, Talbot LJ, Kuo PC. Osteopontin promotes CCL5-mesenchymal stromal cell-mediated breast cancer metastasis. Carcinogenesis. 2011; 32:477–487. [PubMed: 21252118]
17. Jung Y, Kim JK, Shiozawa Y, Wang J, Mishra A, Joseph J, Berry JE, McGee S, Lee E, Sun H, Wang J, Jin T, Zhang H, Dai J, Krebsbach PH, Keller ET, Pienta KJ, Taichman RS. Recruitment of mesenchymal stem cells into prostate tumors promotes metastasis. Nature Communications. 2013; 4:1795.
18. Nagasawa T, Hirota S, Tachibana K, Takakura N, Nishikawa S, Kitamura Y, Yoshida N, Kikutani H, Kishimoto T. Defects of B-cell lymphopoiesis and bone-marrow myelopoiesis in mice lacking the CXC chemokine PBSF/SDF-1. Nature. 1996; 382:635–638. [PubMed: 8757135]
19. Aiuti A, Tavian M, Cipponi A, Ficara F, Zappone E, Hoxie J, Peault B, Bordignon C. Expression of CXCR4, the receptor for stromal cell-derived factor-1 on fetal and adult human lympho-hematopoietic progenitors. European Journal of Immunology. 1999; 29:1823–831. [PubMed: 10382744]
20. Peled A, Petit I, Kollet O, Magid M, Ponomaryov T, Byk T, Nagler A, Ben-Hur H, Many A, Shultz L, Lider O, Alon R, Zipori D, Lapidot T. Dependence of human stem cell engraftment and repopulation of NOD/SCID mice on CXCR4. Science. 1999; 283:845–848. [PubMed: 9933168]
21. Hattori K, Heissig B, Tashiro K, Honjo T, Tateno M, Shieh JH, Hackett NR, Quitoriano MS, Crystal RG, Rafii S, Moore MA. Plasma elevation of stromal cell-derived factor-1 induces mobilization of mature and immature hematopoietic progenitor and stem cells. Blood. 2001; 97:3354–3360. [PubMed: 11369624]
22. Petit I, Szyper-Kravitz M, Nagler A, Lahav M, Peled A, Habler L, Ponomaryov T, Taichman RS, Arenzana-Seisdedos F, Fujii N, Sandbank J, Zipori D, Lapidot T. G-CSF induces stem cell mobilization by decreasing bone marrow SDF-1 and up-regulating CXCR4. Nat Immunol. 2002; 3:687–694. [PubMed: 12068293]
23. Lapidot T, Petit I. Current understanding of stem cell mobilization: The roles of chemokines, proteolytic enzymes, adhesion molecules, cytokines, and stromal cells. Exp Hematol. 2002; 30:973–981. [PubMed: 12225788]
24. Jung Y, Wang J, Schneider A, Sun YX, Koh-Paige AJ, Osman NI, McCauley LK, Taichman RS. Regulation of SDF-1 (CXCL12) production by osteoblasts in the hematopoietic microenvironment and a possible mechanism for stem cell homing. Bone. 2006; 38:497–508. [PubMed: 16337237]
25. Jung Y, Wang J, Song J, Shiozawa Y, Wang J, Havens A, Wang Z, Sun YX, Emerson SG, Krebsbach PH, Taichman RS. Annexin II expressed by osteoblasts and endothelial cells regulates stem cell adhesion, homing, and engraftment following transplantation. Blood. 2007; 110(1):82–90. [PubMed: 17360942]
26. Jung Y, Shiozawa Y, Wang J, Patel LR, Havens AM, Song J, Krebsbach PH, Roodman GD, Taichman RS. Annexin-2 is a regulator of stromal cell-derived factor-1/CXCL12 function in the hematopoietic stem cell endosteal niche. Exp Hematol. 2011; 39(2):151–166. [PubMed: 21108988]
27. Taichman RS, Cooper C, Keller ET, Pienta KJ, Taichman NS, McCauley LK. Use of the stromal cell-derived factor-1/CXCR4 pathway in prostate cancer metastasis to bone. Cancer Res. 2002; 62(6):1832–1837. [PubMed: 11912162]
28. Sun YX, Schneider A, Jung Y, Wang J, Dai J, Wang J, Cook K, Osman NI, Koh-Paige AJ, Shim H, Pienta KJ, Keller ET, McCauley LK, Taichman RS. Skeletal localization and neutralization of the SDF-1(CXCL12)/CXCR4 axis blocks prostate cancer metastasis and growth in osseous sites in vivo. J Bone Miner Res. 2005; 20:318–329. [PubMed: 15647826]
29. Kucia M, Reca R, Miekus K, Wanzeck J, Wojakowski W, Janowska-Wieczorek A, Ratajczak J, Ratajczak MZ. Trafficking of normal stem cells and metastasis of cancer stem cells involve similar mechanisms: Pivotal role of the SDF-1-CXCR4 axis. Stem Cells. 2005; 23:879–894. [PubMed: 15888687]
30. Shiozawa Y, Havens AM, Jung Y, Ziegler AM, Pedersen EA, Wang J, Wang J, Lu G, Roodman GD, Loberg RD, Pienta KJ, Taichman RS. Annexin II/annexin II receptor axis regulates adhesion,

migration, homing, and growth of prostate cancer. J Cell Biochem. 2008; 105(2):370–380. [PubMed: 18636554]

31. Lehr JE, Pienta KJ. Preferential adhesion of prostate cancer cells to a human bone marrow endothelial cell line. J Natl Cancer Inst. 1998; 90:118–123. [PubMed: 9450571]
32. Ling Q, Jacovina AT, Deora A, Febbraio M, Simantov R, Silverstein RL, Hempstead B, Mark WH, Hajjar KA. Annexin II regulates fibrin homeostasis and neoangiogenesis in vivo. J Clin Invest. 2004; 113:38–48. [PubMed: 14702107]
33. Scotton CJ, Wilson JL, Scott K, Stamp G, Wilbanks GD, Fricker S, Bridger G, Balkwill FR. Multiple actions of the chemokine CXCL12 on epithelial tumor cells in human ovarian cancer. Cancer Res. 2002; 62:5930–5938. [PubMed: 12384559]
34. Hartmann TN, Burger JA, Glodek A, Fujii N, Burger M. CXCR4 chemokine receptor and integrin signaling co-operate in mediating adhesion and chemoresistance in small cell lung cancer (SCLC) cells. Oncogene. 2005; 24:4462–4471. [PubMed: 15806155]
35. Katayama A, Ogino T, Bandoh N, Nonaka S, Harabuchi Y. Expression of CXCR4 and its down-regulation by IFN-gamma in head and neck squamous cell carcinoma. Clin Cancer Res. 2005; 11:2937–2946. [PubMed: 15837745]
36. Marchesi F, Monti P, Leone BE, Zerbi A, Vecchi A, Piemonti L, Mantovani A, Allavena P. Increased survival, proliferation, and migration in metastatic human pancreatic tumor cells expressing functional CXCR4. Cancer Res. 2004; 64:8420–8427. [PubMed: 15548713]
37. Darash-Yahana M, Pikarsky E, Abramovitch R, Zeira E, Pal B, Karplus R, Beider K, Avniel S, Kasem S, Galun E, Peled A. Role of high expression levels of CXCR4 in tumor growth, vascularization, and metastasis. FASEB J. 2004; 18:1240–1242. [PubMed: 15180966]
38. Sun YX, Wang J, Shelburne CE, Lopatin DE, Chinnaiyan AM, Rubin MA, Pienta KJ, Taichman RS. Expression of CXCR4 and CXCL12 (SDF-1) in human prostate cancers (PCa) in vivo. J Cell Biochem. 2003; 89(3):462–473. [PubMed: 12761880]
39. Kryczek I, Wei S, Keller E, Liu R, Zou W. Stroma-derived factor (SDF-1/CXCL12) and human tumor pathogenesis. Am J Physiol Cell Physiol. 2007; 292:C987–C995. [PubMed: 16943240]
40. Genetos DC, Wong A, Watari S, Yellowley CE. Hypoxia increase Annexin A2 expression in osteoblastic cells via VEGF and ERK. Bone. 2010; 47(6):1013–1019. [PubMed: 20817051]
41. Gillette JM, Nielsen-Preiss SM. The role of annexin 2 in osteoblastic mineralization. J Cell Sci. 2004; 117(3):441–449. [PubMed: 14679310]
42. Zhuang Q, Li J, Wu Z, Zhang J, Sun W, Li T, Yan Y, Jiang Y, Zhao RC, Qiu G. Differential proteome analysis of bone marrow mesenchymal stem cells from adolescent idiopathic scoliosis patients. PLoS ONE. 2011; 6(4):e18834. [PubMed: 21526124]
43. Helbig G, Christopherson KW 2nd, Bhat-Nakshatri P, Kumar S, Kishimoto H, Miller KD, Broxmeyer HE, Nakshatri H. NF-kB promotes breast cancer cell migration and metastasis by inducing the expression of the chemokine receptor CXCR4. J Biol Chem. 2003; 278:21631–21638. [PubMed: 12690099]
44. Rehman AO, Wang CY. SDF-1-Promotes Invasion of head and neck squamous cell carcinoma by activating NF-kB. J Biol Chem. 2008; 283(29):19888–19894. [PubMed: 18448428]
45. Kukreja P, Abdel-Mageed AB, Mondal D, Liu K, Agrawal KC. Up-regulation of CXCR4 expression in PC-3 cells by stromal-derived factor-1 (CXCL12) increases endothelial adhesion and transendothelial migration: role of MEK/ERK signaling pathway-dependent NF-kB activation. Cancer Res. 2005; 65:9891–9898. [PubMed: 16267013]
46. Sharma MR, Koltowski L, Ownbey RT, Tuszynski GP, Sharma MC. Angiogenesis-associated protein annexin II in breast cancer: selective expression in invasive breast cancer and contribution to tumor invasion and progression. Exp Mol Path. 2006; 81:146–156. [PubMed: 16643892]
47. Sharma M, Blackman MR, Sharma MC. Antibody-directed neutralization of annexin II (ANX II) inhibits neoangiogenesis and human breast tumor growth in a xenograft model. Exp Mol Path. 2012; 92:175–184. [PubMed: 22044461]
48. Wang JH, Wang J, Sun Y-X, Song W, Nor J, Wang CY, Taichman RS. Diverse signaling pathways through the SDF-1/CXCR4 chemokine axis in prostate cancer cell lines leads to altered patterns of cytokine secretion and angiogenesis. Cellular Signalling. 2005; 17(12):1578–1592. [PubMed: 16005185]

49. Wang J, Loberg R, Taichman RS. The pivotal role of CXCL12 (SDF-1)/CXCR4 axis in bone metastasis. Cancer Metastasis Rev. 2006; 25(4):573–587. [PubMed: 17165132]

50. Wang J, Wang J, Dai J, Jung Y, Wei CL, Wang Y, Havens AM, Hogg PJ, Keller ET, Pienta KJ, Nor JE, Wang CY, Taichman RS. A glycolytic mechanism regulating an angiogenic switch in prostate cancer. Cancer Res. 2007; 67(1):149–159. [PubMed: 17210694]

51. Rempel SA, Dudas S, Ge S, Gutierrez JA. Identification and localization of the cytokine SDF1 and its receptor, CXC chemokine receptor 4, to regions of necrosis and angiogenesis in human glioblastoma. Clin Cancer Res. 2000; 6:102–111. [PubMed: 10656438]

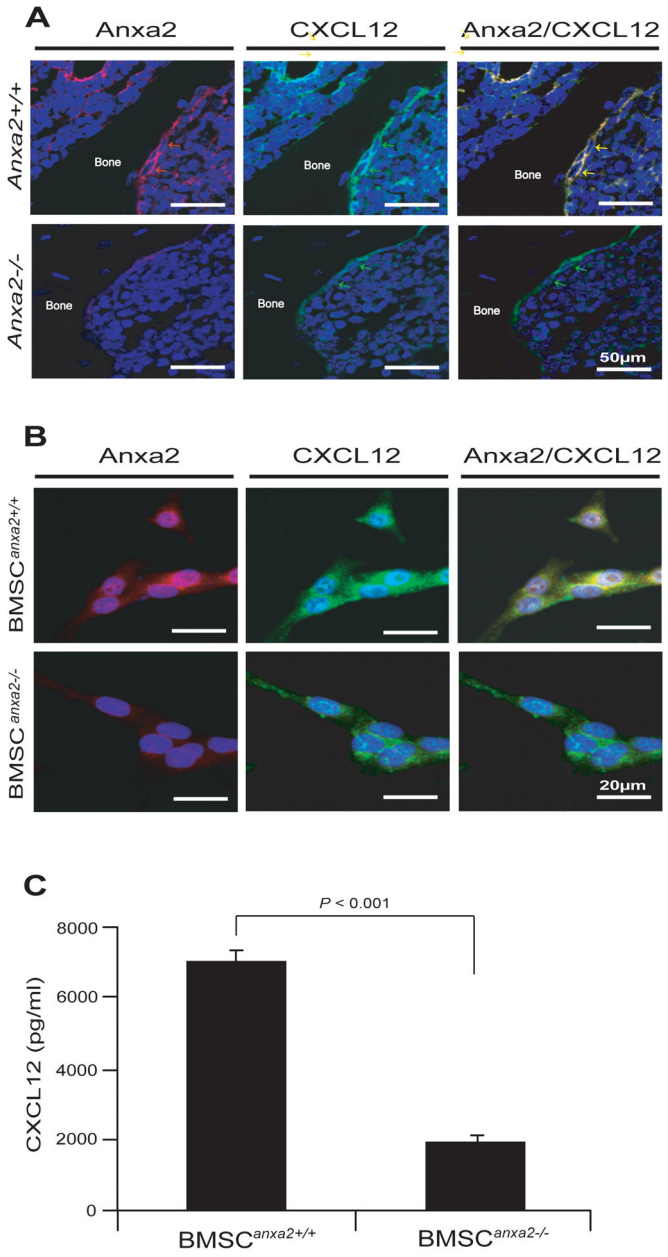

Figure 1. ANXA2 expression is co-localized with CXCL12 expression in BMSCs in marrow

(**A**) Expression of ANXA2 (red arrows) and CXCL12 (green arrows) in osteoblasts on the long bones of wild-type and *Anxa2* knocked-out mice as detected by immunofluorescence staining. Yellow arrows; colocalization of ANXA2 and CXCL12 on osteoblasts. Blue; DAPI nuclear stain. BAR = 50μm. (**B**) Expression of ANXA2 (red) and CXCL12 (green) by BMSC$^{Anxa2+/+}$ or BMSC$^{Anxa2-/-}$ as detected by immunofluorescence staining. Blue, DAPI nuclear stain. BAR = 20μm. (**C**) Secretion of CXCL12 by BMSC$^{Anxa2+/+}$ or BMSC$^{Anxa2-/-}$ as determined by ELISA. Data are representative of mean with s.d. for triplicates in each of three independent experiments (Student's *t*-test).

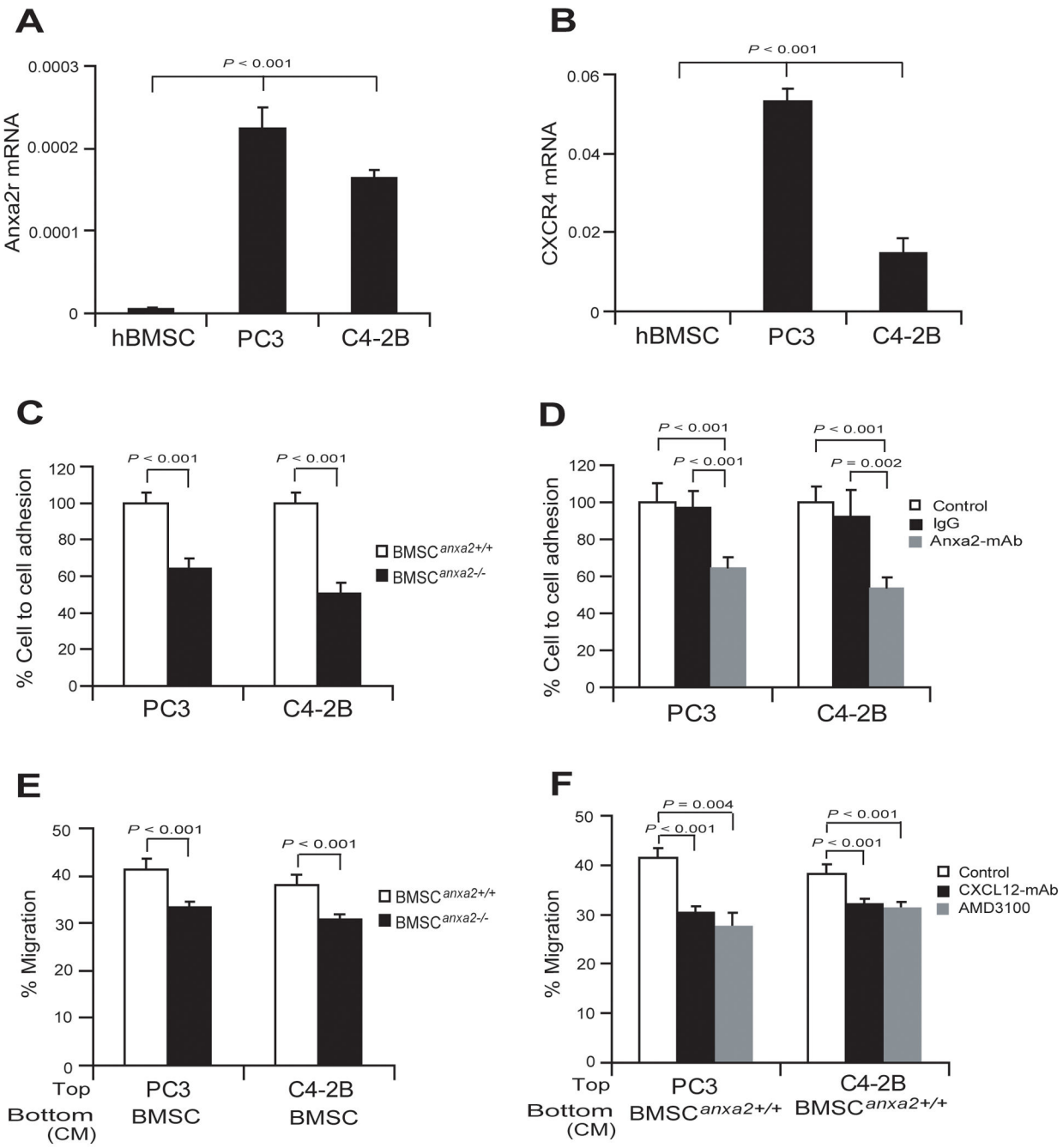

Figure 2. ANXA2 and CXCL12 interact to regulate PCa cell adhesion and migration

(**A**) Expression of mRNA for the ANXA2 receptor (*Anxa2r*) by PCa cells (PC3 or C4-2B) determined by real-time RT-PCR. hBMSCs were used as negative controls. (**B**) Expression of mRNA for the CXCL12 receptor, *Cxcr4* by PCa cells (PC3 or C4-2B). hBMSCs were used as negative controls. (**C**) Adhesion of PCa cells to BMSCs expressing different levels of ANXA2. Adhesion was determined by quantifying the number of CFDA stained PCa cells bound to BMSC, with binding to $BMSC^{Anxa2+/+}$ set at 100%. (**D**) Adhesion of PCa cells to BMSCs with the presence or absence of a functional blocking antibody to ANXA2.

IgG matched control was used as an antibody control. (**E**) Migration of PCa cells (PC3 or C4-2B) towards CM derived from BMSC$^{Anxa2+/+}$ or BMSC$^{Anxa2-/-}$ was performed in Transwell® plates, where % migration was set at 100% for the initial cell numbers in top chamber. (**F**) Migration of PCa cells to BMSCs in the presence of neutralizing anti-CXCL12 antibody or AMD3100, a selective CXCR4 antagonist. Data are representative of mean with s.d. for triplicates in each of three independent experiments (Student's *t*-test).

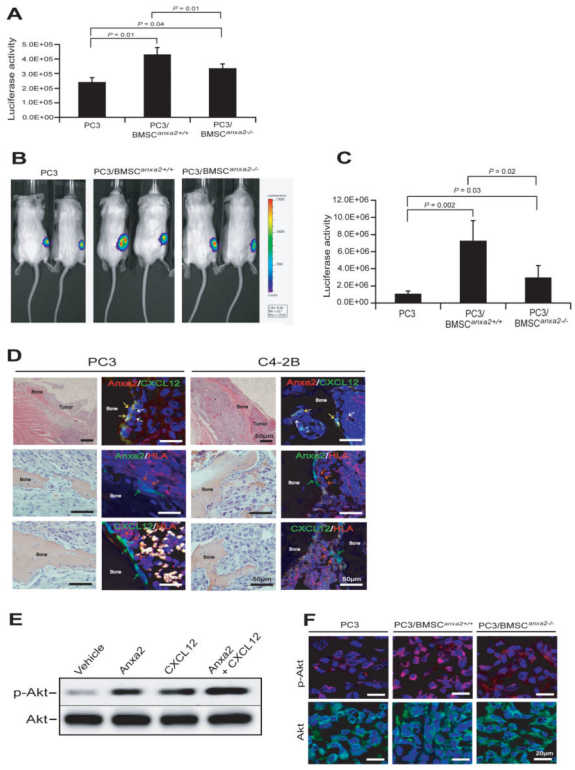

Figure 3. ANXA2 and CXCL12 interact to regulate PCa cell growth

(**A**) PC3^{Luc} cells were placed in co-culture with BMSC$^{Anxa2+/+}$ or BMSC$^{Anxa2-/-}$, and proliferation was evaluated at 48 hours by determining the change in luciferase levels using a Dual-Luciferase Reportor Assay kit. Data are representative of mean with s.d. for triplicates in each of three independent experiments (Student's *t*-test). (**B, C**) SCID mice were implanted *s.c.* PC3^{luc} cells alone or mixed with BMSC$^{Anxa2+/+}$ or BMSC$^{Anxa2-/-}$. Tumor growth was evaluated by BLI imaging at 5 weeks (n=5 animals/group, mean±s.d., Student's *t*-test). (**D**) SCID mice were implanted *i.t.* with PC3^{luc} or C4-2B^{luc} to directly test tumor growth in bone marrow. H&E staining demonstrates tumor growth in marrow (left panels). BAR = 50μm. Co-localization of ANXA2 and CXCL12 on osteoblasts (yellow arrows) associated with the bone surface was detected by immunofluorescence staining (top right panels). Blue; DAPI nuclear stain. BAR = 50μm. HLA-positive tumor cells (red arrows) are associated with ANXA2 (green arrows) expressing obstoblasts (middle right panels) or CXCL12 (green arrows) expressing obstoblasts (bottom right panels) as detected by immunofluorescence staining. BAR = 50μm. (**D**) ANXA2, CXCL12 or a combination of ANXA2 and CXCL12 were treated to PC3 cells for 30 min. Western blot was performed to detect p-AKT or AKT levels. (**F**) Immunofluorescence staining of p-AKT or AKT on the tumors generated in Fig. 3B.

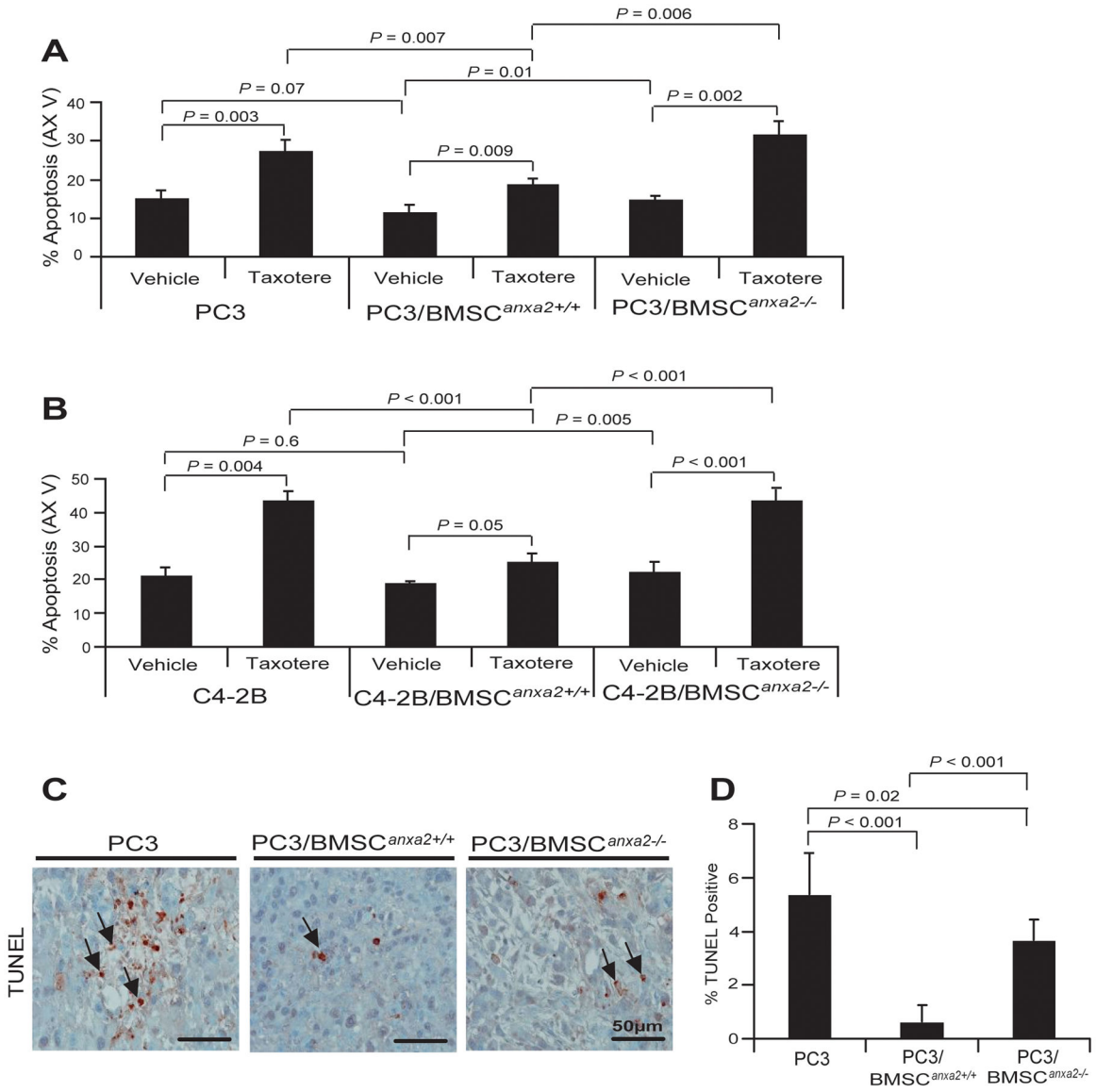

Figure 4. ANXA2 and CXCL12 in the marrow environment enhance PCa survival and drug-resistance

PC3^{GFP} or C4-2B^{GFP} cells were directly cultured with BMSC$^{Anxa2+/+}$ or BMSC$^{Anxa2-/-}$ for 48 hours and taxotere was introduced into the culture for an additional 48 hours. Annexin V staining was performed on the recovered (**A**) PC3 or (**B**) C4-2B cells and quantified by FACS. Data in (Fig. 4A and B) are representative of mean with s.d. for triplicates in each of three independent experiments (Student's *t*-test). (**C**) TUNEL staining of apoptotic PCa cells (black arrows) of tumors grown from PC3^{luc} cells alone or mixed with BMSC$^{Anxa2+/+}$ or BMSC$^{Anxa2-/-}$ implanted into SCID mice. BAR = 50μm. (**D**) Quantification of % TUNEL positive cells in Fig. 4C (mean±s.d., Student's *t*-test).

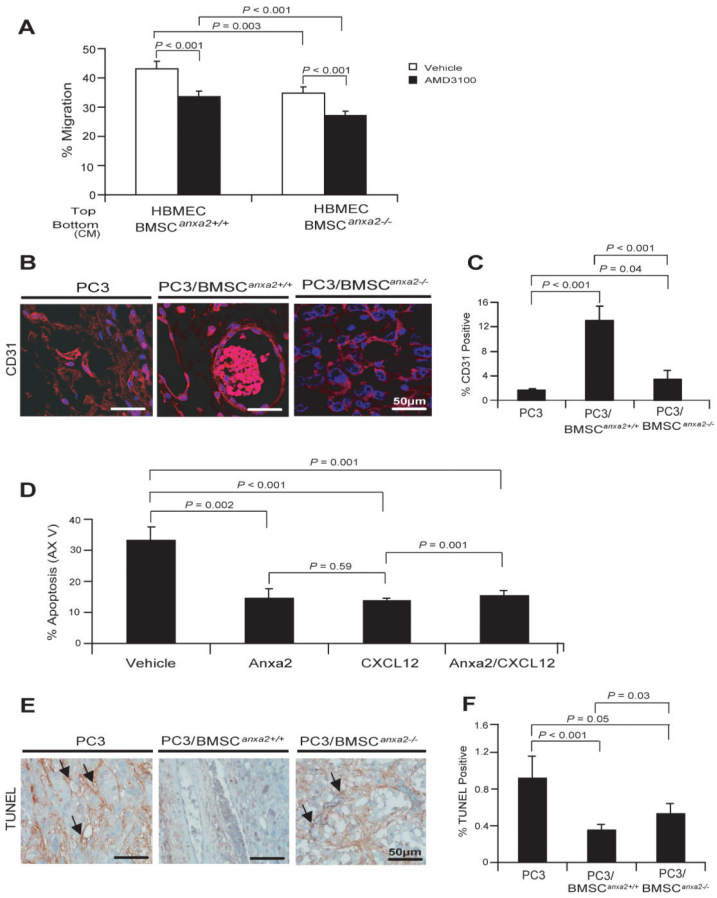

Figure 5. ANXA2 and CXCL12 expression by BMSCs increases vascular formation

(**A**) Migration of HBMEC towards CM isolated from BMSC$^{Anxa2+/+}$ or BMSC$^{Anxa2-/-}$. Migration assays of HBMEC were performed in Transwell® plates using CM from BMSC$^{Anxa2+/+}$ or BMSC$^{Anxa2-/-}$ with and without AMD3100, a selective CXCR4 antagonist. Data are representative of mean with s.d. for triplicates in each of three independent experiments (Student's *t*-test). (**B**) CD31 staining (red) for blood vessel cells in tumors grown from PC3^{luc} cells alone or mixed with BMSC$^{Anxa2+/+}$ or BMSC$^{Anxa2-/-}$ implanted into SCID mice. Blue, DAPI nuclear stain. Bar = 50μm. (**C**) Quantification of % CD31 positive cells in Figure 5B (mean±s.d., Student's *t*-test). (**D**) Apoptotic HBMEC cells in the presence of ANXA2, CXCL12 or combination of ANXA2 and CXCL12 were quantified by FACS analysis using Annexin V staining. Data are representative of mean with s.d. for triplicate determinations in each of three independent experiments (Student's *t*-test). (**E**) TUNEL staining of apoptotic endothelial cells (black arrows) in tumors grown from PC3^{luc} cells mixed with BMSC$^{Anxa2+/+}$ or BMSC$^{Anxa2-/-}$ implanted into SCID mice. BAR = 50μm. (**F**) Quantification of % TUNEL positive cells in Fig. 5E (mean±s.d., Student's *t*-test).